Cellular automaton simulation of pedestrian counter flow with different walk velocities

W. G. Weng, T. Chen, H. Y. Yuan, and W. C. Fan

Center for Public Safety Research, Department of Engineering Physics, Tsinghua University, Beijing, 100084, Peoples Republic of China

(Received 22 January 2006; revised manuscript received 29 May 2006; published 5 September 2006)

This paper presents a cellular automaton model without step back for pedestrian dynamics considering the human behaviors which can make judgments in some complex situations. This model can simulate pedestrian movement with different walk velocities through update at different time-step intervals. Two kinds of boundary conditions including periodic and open boundary for pedestrian counter flow are considered, and their dynamical characteristics are discussed. Simulation results show that for periodic boundary condition there are three phases of pedestrian patterns, i.e., freely moving phase, lane formation phase, and perfectly stopped phase at some certain total density ranges. In the stage of lane formation, the phenomenon that pedestrians exceed those with lower walk velocity through a narrow walkway can be found. For open boundary condition, at some certain entrance densities, there are two steady states of pedestrian patterns; but the first is metastable. Spontaneous fluctuations can break the first steady state, i.e., freely moving phase, and run into the second steady state, i.e., perfectly stopped phase.

DOI: 10.1103/PhysRevE.74.036102 PACS number(s): 89.40.−a, 05.65.+b, 45.40.Ln, 84.35.+i

I. INTRODUCTION

Recently, cellular automata (CA) have been extensively used for modeling complex phenomena in various fields such as fluid dynamics, statistical physics, biology, and other complex systems [1]. As an important class of models, CA have attracted much attention as a model for dynamics of traffic flow [2–4]. On the other hand, pedestrian dynamics has not been studied as extensively as vehicular traffic, especially using a CA approach, and up to now studies on this topic are very scarce [5–16]. The reason may be that the pedestrian movement is more complex than vehicular flow [13,14]. First, pedestrians are more intelligent than vehicles and they can choose an optimum route according to the environment around. Secondly, pedestrians are more flexible in changing directions and not limited to the "lanes" as in vehicular flow. Thirdly, the slight bumping is acceptable and need not be absolutely avoided as in traffic flow models. So the model developed for pedestrian movement should fully consider these differences in order to study the special phenomena in pedestrian dynamics. It is a pity that till now, it is not enough to understand pedestrian dynamics, especially for the condition of different walk velocities, though it has many models considering the special characteristics of pedestrian movement.

Pedestrian movement is an important component in the analysis and design of transportation facilities, pedestrian walkways, traffic intersections, markets, and other public buildings. Continuum models have been successful in modeling pedestrian dynamics, and many interesting collective effects and self-organization phenomena have been observed, e.g., jamming and clogging, lane formation, and oscillations at bottlenecks in counter flow or collective patterns of motion at intersections [17–20]. An important example is the social force model [18,19]. Here pedestrians are treated as particles subject to long-ranged forces induced by the social behavior of the individuals. This leads to (coupled) equations of motion similar to Newtonian mechanics.

CA for pedestrian dynamics have been proposed in Refs. [5–13] and Refs. [14–16]. The models in the former references can be considered as generalizations of the Biham-Middleton-Levine model for city traffic [21], and named as biased random walker model. The latter ones introduce floor field which modifies the transition rates to neighbor cells, inspired from the process of chemotaxis as used by some insects.

In this paper, a cellular automaton model without step back for pedestrian dynamics considering the human behaviors which can make judgment in some complex situations is proposed. This model can simulate pedestrian movement with different walk velocities through update at different time-step intervals. Two kinds of boundary conditions including periodic and open boundary for pedestrian counter flow are considered, and their dynamical characteristics are discussed. In the following section, model and boundary conditions are presented. Section III gives simulation results and discussions, followed by conclusions.

II. MODEL AND BOUNDARY CONDITIONS

We describe the cellular automaton model for the pedestrian counter flow in a two-dimensional system. The underlying structure is a $W \times W$ cell grid, where W is the system size. Each cell can either be empty, or occupied by wall or exactly one pedestrian. For simulating the pedestrian movement with different walk velocities, Kirchner *et al.* investigated the influence of the interaction range and the spatial discretization [22]. For the former one, they simulated pedestrian movement through letting pedestrian move more than one cell. And for the latter one, they combined with a reduction of the cell size to study the effect of small move distance at one time step. But in their pedestrian simulation, there is only one kind of pedestrian, i.e., all pedestrians with the same walk velocity in spite of high or small walk velocity. Actually in one pedestrian system, there are many walk velocities for different pedestrians. In this paper, we introduce a new idea for simulating pedestrian movement with different walk velocities, i.e., pedestrians update at different time-step intervals. For example, for the pedestrians with walk veloci-

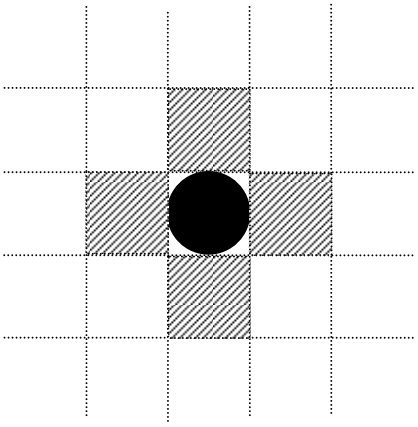

FIG. 1. Von Neumann neighbor setup in a two-dimensional rectangular grid.

ties of 1.0 and 1.5 m/s, the former ones update at every 3 time steps, and the latter ones are at every 2 time steps, if the size of a cell corresponds to approximately 0.4×0.4 m^2 and one time-step is approximately 2/15 s.

In CA, a rule defines the state of a cell in dependence of the neighbor of the cell. In this model, the Von Neumann neighbor setup shown in Fig. 1 is used. Thus, the state of the core cell at the next update time step depends on the states of the cells in the neighbor including the cell above, below, right and left, also the core cell itself, of this update time step.

In this model, there are four kinds of walkers including the right walkers with walk velocities of 1.0 and 1.5 m/s moving from the left to the right boundary, and the left walkers with walk velocities of 1.0 and 1.5 m/s moving from the right to the left boundary. Each walker moves to the preferential direction with no back step. Figure 2 shows all the possible configurations of the right walker with walk velocity of 1.0 m/s (going to the right). The nomenclature of "*P*" is the transition probabilities to the nearest-neighbor sites, and the subscripts "*a*," "*b*," and "*w*" means the above, bottom, and waiting labels, respectively. In Fig. 2(a), the right adjacent cell is unoccupied; the right walker will move right independent of the state of the above and below adjacent cells. But if the right adjacent cell is occupied, his route choice depends on the state of the above and below adjacent cells. In Figs. 2(b)–2(d), the right adjacent cell is occupied by the right walker with walk velocity more than or equal to his walk velocity; in Figs. 2(e)–2(g), the occupied right adjacent cell is the left walker. For configurations (e)–(g), we consider the traffic rule. The pedestrian is obligated to walk on the right-hand side of the walkway in China. The walker has the priority to move on the right-hand side of the walkway. Therefore, we introduce the following traffic rule for the transition probabilities of the walker: the walker moves preferably to the right-hand direction in the configurations (e)–(g), i.e., $P_{b21}>P_{a21}$ and $P_{b22}>P_{a23}$. For configuration (h), if the above, below and right adjacent cells are all occupied, the right walker will have to stop and wait.

If the considered right walker has the walk velocity of 1.5 m/s, a question of exceeding another right walker with lower walk velocity occurs. Figure 3 gives the adding pos-

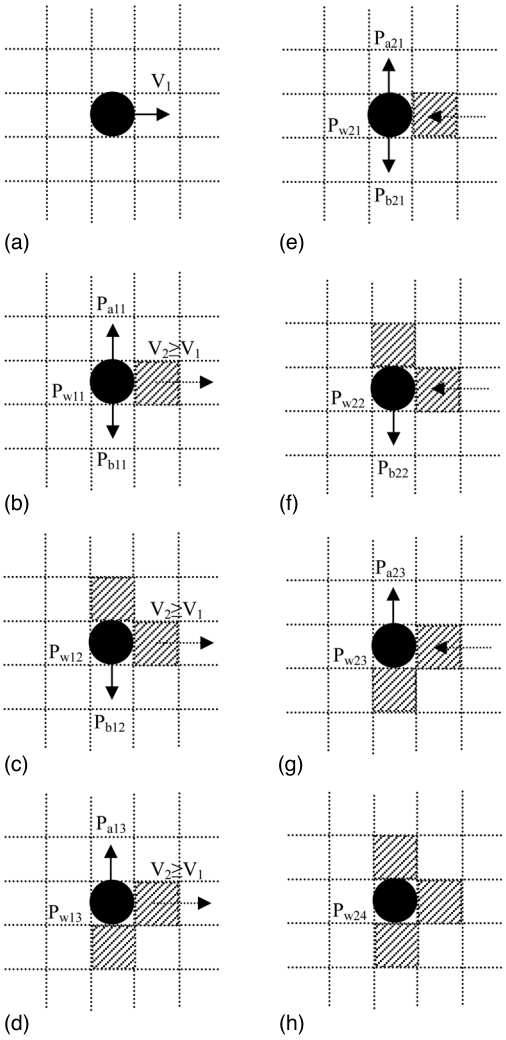

FIG. 2. (a)–(h) All the possible configurations of the right walker with walk velocity of 1.0 m/s (going to the right). The arrow in the right adjacent cell indicates the moving direction of the walker in that cell. The arrow from the core cell indicates the possible direction of the right walker in the core cell may select. The nomenclature of "*P*" is the transition probabilities to the nearest-neighbor sites, and the subscripts of "*a*," "*b*," and "*w*" means the above, bottom, and waiting labels, respectively.

sible configurations of the right walker with walk velocity of 1.5 m/s next to those in Fig. 2. Chinese are accustomed to exceeding another pedestrian with lower walk velocity from the left-hand side. So in Fig. 3, $P_{a31}>P_{b31}$ and $P_{a33}>P_{b32}$. In other countries where the pedestrians prefer to walk on the left-hand side of walkway and exceed from the right-hand side, the contrary rules can be adopted accordingly. In the same way, we can define the similar treatment for the possible configurations that the left walkers with walk velocities of 1.0 and 1.5 m/s may encounter.

In this model, sequential update is chosen (named shuffled update in Ref. [23]) since pedestrian dynamics in two dimensions is intrinsically stochastic, and also this case is nontrivial. In each update time-step, the pedestrians are numbered randomly from 1 to *N*, where *N* is the total number of pedestrians in the system, and then each pedestrian is

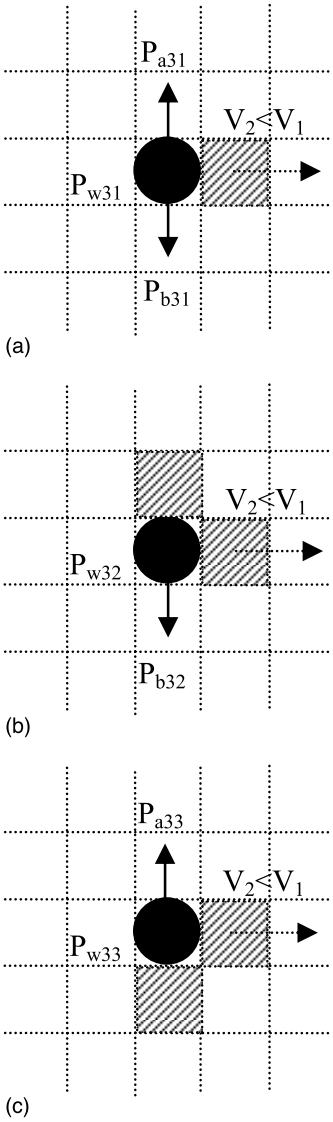

FIG. 3. (a)–(c) Adding possible configurations of the right walker with walk velocity of 1.5 m/s to those in Fig. 2.

updated once in the sequential order from 1 to N.

Figure 4 shows the schematic illustration of the pedestrian counter flow in the system, which is composed of the top and bottom walls. The right walkers going to the right with walk velocities of 1.0 and 1.5 m/s are indicated by the white and black full circles, respectively; and the left ones with walk velocities of 1.0 and 1.5 m/s are indicated by the red and green ones. Here we consider two boundary conditions including periodic and open boundary. For the periodic boundary condition, the pedestrians of four types are initially distributed randomly. If the right walker arrives at the right boundary, he moves to the left boundary; if the left walker arrives at the left boundary, he moves to the right boundary. Thus, the total number of walkers of each type is conserved as $p_{\mathrm{plr}}W^2$, $p_{phr}W^2$, $p_{pll}W^2$, and $p_{phl}W^2$, where p_{plr}, p_{phr}, p_{pll}, and p_{phl} are the initial densities for white, black, red, and green ones (representing right walker with lower velocity, right walker with higher velocity, left walker with lower velocity, and left walker with high velocity, respectively). The

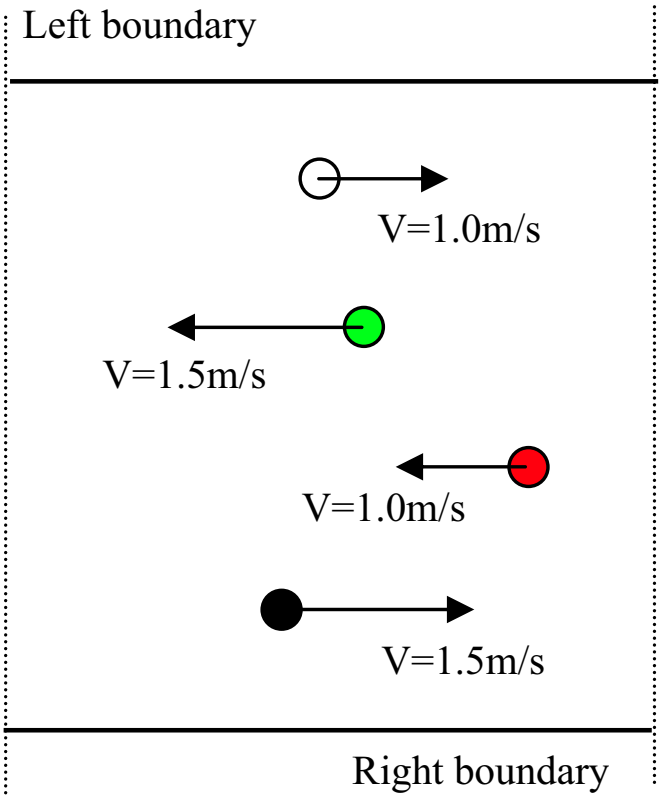

FIG. 4. (Color online) Schematic illustration of the pedestrian counter flow in the system, which is composed of top and bottom walls. The white and black full circles indicate the right walkers (going to the right) with walk velocities of 1.0 and 1.5 m/s, respectively. The red and green full circles are the left walkers with walk velocities of 1.0 and 1.5 m/s, respectively.

total density is $p_p=p_{plr}+p_{phr}+p_{pll}+p_{phl}$; and only $p_{plr}=p_{phr}=p_{pll}=p_{phl}$ is considered in this paper. For the open boundary condition, the right walkers of walk velocities of 1.0 m/s with number of $p_{olr}W$, and 1.5 m/s with number of $p_{ohr}W$ are distributed randomly on the left boundary at every 6 time steps. Similarly, the left walkers with numbers of $p_{oll}W$ and $p_{ohl}W$ are distributed randomly on the right boundary at every 6 time steps. If the right walkers arrive at the right boundary, and the left ones arrive at the left boundary, they are removed from the system. In this paper, only $p_{olr}=p_{ohr}=p_{oll}=p_{ohl}=p_o/2$ is considered, where p_{olr}, p_{ohr}, p_{oll}, and p_{ohl} are the entrance densities for white, black, red, and green ones, and p_o is the entrance density of walkers of each boundary.

III. SIMULATION RESULTS AND DISCUSSIONS

Using the model and boundary conditions described above, we carried out the simulation for pedestrian counter flow. The system size is set to be $W=60$. Considering the traffic rule and custom, the transition probabilities are $P_{a11}=P_{b11}=0.25$, $P_{w11}=0.50$; $P_{b12}=p_{w12}=0.50$; $P_{a13}=p_{w13}=0.50$; $P_{a21}=0.10$, $P_{b21}=0.40$, $P_{w21}=0.50$; $P_{b22}=P_{w22}=0.50$; $P_{a23}=0.10$, $P_{w23}=0.90$; $P_{w24}=1.00$; $P_{a31}=0.40$, $P_{b31}=0.10$, $P_{w31}=0.50$; $P_{b32}=0.10$, $P_{w32}=0.90$; $P_{a33}=0.90$, $P_{w33}=0.10$.

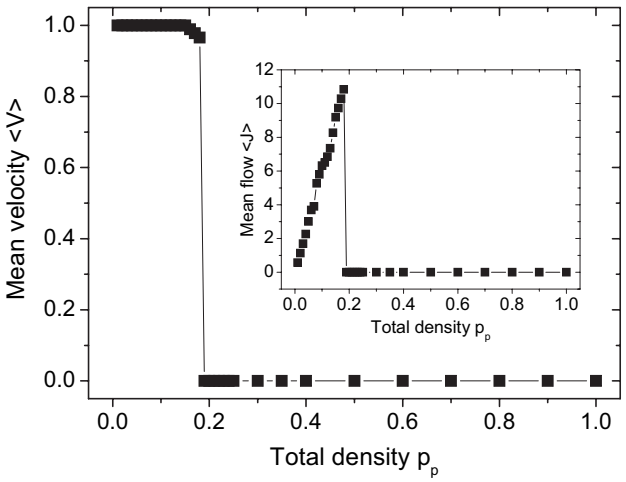

FIG. 5. Plot of the mean velocity $\langle V\rangle$ and the mean flow $\langle J\rangle$ against the total density p_p for the system size $W=60$ in the pedestrian counter flow with periodic boundary condition.

For the periodic boundary condition, we check the mean velocity $\langle V\rangle$ and the mean flow $\langle J\rangle$ of pedestrian counter flow. The mean velocity $\langle V\rangle$ of pedestrians moving at one update time step is defined as the value of the number of walkers moving forward divided by the total number of walkers existing in the system $N(=p_pW^2)$. The mean flow $\langle J\rangle$ of pedestrians is defined as the sum of the number of the right walkers moving through the right boundary and that of the left ones moving through the left boundary at one update time step. For each simulation, 20 000 time steps are carried out, and the value of $\langle V\rangle$ and $\langle J\rangle$ are computed according to the last 4000 time steps averaged over 10 different random initial pedestrian distributions, although in all of our simulations it takes no more than 10 000 time steps to reach the steady states.

Figure 5 gives the plot of the mean velocity $\langle V\rangle$ and the mean flow $\langle J\rangle$ against the total density p_p for the system size $W=60$ in the pedestrian counter flow with periodic boundary condition. Figure 6 shows the pedestrian patterns obtained at time step=20 000, (a) the freely moving phase obtained at $p_p=0.04$; (b) the lane formation phase obtained at $p_p=0.15$; (c) the perfectly stopped phase obtained at $p_p=0.40$. From Figs. 5 and 6, it is indicated that with the increasing total density, there are three phases of pedestrian patterns, i.e., freely moving phase, lane formation phase and perfectly stopped phase. The critical total densities are $p_{pcr1}=0.078\pm0.005$ and $p_{pcr2}=0.183\pm0.005$, which are averaged over 10 random initial pedestrian distributions. In the situation of $p_p<p_{pcr1}$, all of the walkers can move freely, i.e., $\langle V\rangle=1$. But when $p_p\geqslant p_{pcr2}$, none of the walkers can move forward, i.e., $\langle V\rangle=0$ and $\langle J\rangle=0$. Here it should be noted that it is not easy to determine when a lane is formed in the background of freely moving pedestrians. We only estimate if a lane forms through observing the pedestrian pattern obtained at time step=20 000. Obviously, the critical total densities depend on the system size W [13], and the initial pedestrian distribution. In our simulations, different initial pedestrian distributions may result in different number of

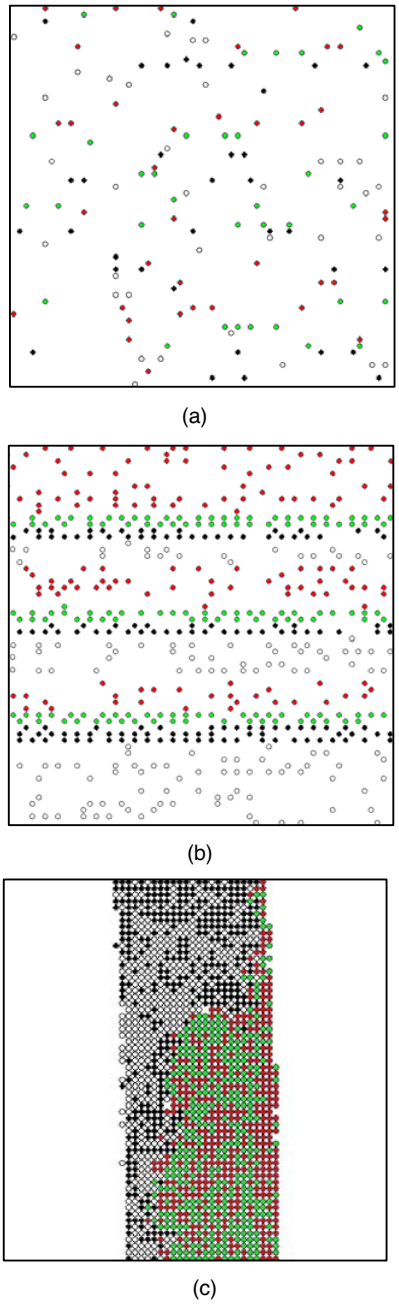

FIG. 6. (Color online) Pedestrian patterns obtained at time step=20 000 for the system size $W=60$, (a) the freely moving phase obtained at $p_p=0.04$; (b) the lane formation phase obtained at $p_p=0.15$; (c) the perfectly stopped phase obtained at $p_p=0.40$.

lanes though it has the same total density, the reason of which is unclear and should be studied further.

In the stage of lane formation (the total density $p_p\in[0.078,0.183)$), with the increasing total density from 0.15 to 0.18 in Fig. 6, $\langle V\rangle$ decreases slightly, but $\langle J\rangle$ increases all the while. Figure 6(b) shows the empirically confirmed development of dynamically varying lanes consisting of pedestrians who intend to walk in the same walk direction and with the same walk velocity. Periodic boundary condition in the transversal direction would form and stabilize these lanes since they would no longer be destroyed at the ends of the

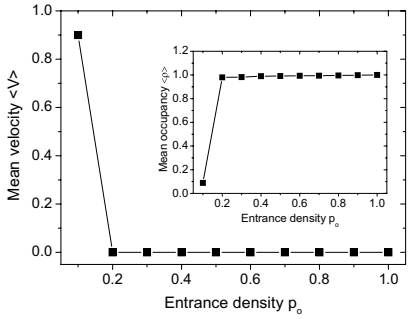

FIG. 7. Plot of the mean velocity $\langle V\rangle$ and the mean occupancy $\langle\rho\rangle$ against the entrance density p_o for the system size $W=60$ in the pedestrian counter flow with open boundary condition.

walkway by entering pedestrians. The segregation effect of lane formation is not only a result of the initial pedestrian distribution but also a consequence of the pedestrians' interactions. Pedestrians moving in a mixed crowd or moving against the stream will have frequent and strong interactions. In each interaction, the encountering pedestrians move a little aside according to traffic rule and custom in order to pass each other. This sidewards movement tends to separate oppositely moving pedestrians and those with different walk velocities. Moreover, once the pedestrians move in uniform lanes, they will have very rare and weak interactions. Hence, the tendency to break up existing lanes is negligible [20]. Simulations show that group lane composed of four lanes of pedestrians of different walk directions and velocities is always formed. Another interesting phenomenon from Fig. 6(b) is that the lane of pedestrians with higher walk velocity is narrower than that of pedestrians with lower walk velocity which can also be found in experiments of pedestrian walking in rush hour in underground station [24]. The reason is that pedestrians with higher walk velocity have more chances for update than those with lower walk velocity. When pedestrians with higher walk velocity encounter those with lower walk velocity, they may move aside, but those with lower walk velocity have more probability to wait. Therefore, the way of higher walk velocity is narrower than that of lower walk velocity by a large number of time steps.

From the above analysis, it is indicated that with the periodic boundary condition, we can simulate some typical phenomena observed empirically such as lane formation and jamming using this presented model, whose update rules are obviously simpler than those of floor field model [14–16] and continuous model [19,20].

For the open boundary condition, we check the mean velocity $\langle V\rangle$ and the mean occupancy $\langle\rho\rangle$ of pedestrian counter flow. The definition of $\langle V\rangle$ here is the same as that for the periodic boundary condition described above. The mean occupancy $\langle\rho\rangle$ of pedestrians is defined as the fraction of sites occupied by the walkers. For each simulation, 20 000 time steps are also carried out, and the value of $\langle V\rangle$ and $\langle\rho\rangle$ are computed according to the last 4000 time steps averaged over 10 different random pedestrian distributions in the entrances of boundaries, although in all of our simulations it takes no more than 10 000 time steps to reach the steady states.

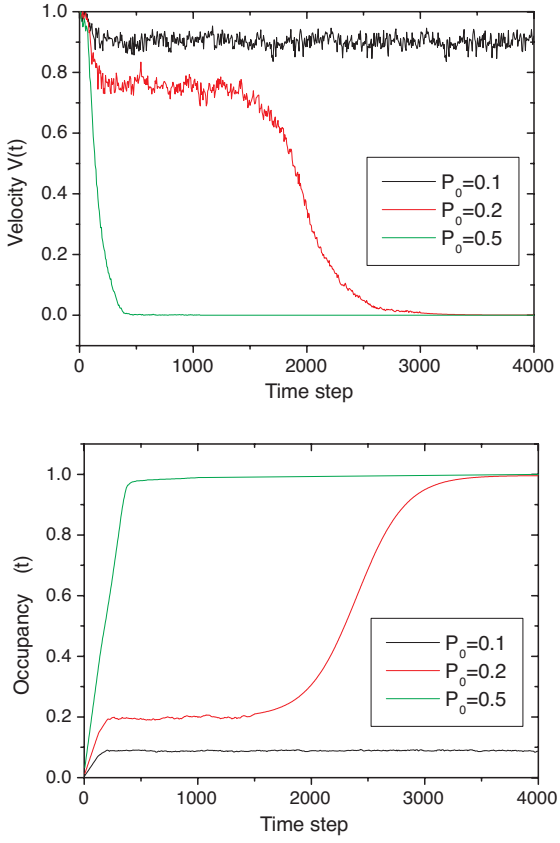

FIG. 8. (Color online) Time evolution of (a) the velocity $V(t)$ and (b) the occupancy $p(t)$ for the system size $W=60$ in the pedestrian counter flow with open boundary condition at the entrance density $p_o=0.1$, 0.2, and 0.5.

Figure 7 shows the plot of the mean velocity $\langle V\rangle$ and the mean occupancy $\langle\rho\rangle$ against the entrance density p_o for the system size $W=60$ in the pedestrian counter flow with open boundary condition. Not like periodic boundary condition, the lane with open boundary condition in the system size $W=60$ does not form because it is destroyed by randomly entering pedestrians and can not be stabilized; only the freely moving phase and perfectly stopped phase come into being. It is indicated from Fig. 7 that with the increase of the entrance density p_o, the mean velocity $\langle V\rangle$ decreases, and the mean occupancy $\langle\rho\rangle$ increases. When p_o is larger than the critical value (here $p_{ocr}=0.12\pm0.01$ for the system size $W=60$ for simulation results), $\langle V\rangle$ becomes zero and $\langle\rho\rangle$ goes to 1.0. The critical value of occupancy at the critical entrance density is given by $\langle\rho_{cr}\rangle=0.19\pm0.01$ obtained from simulations. Here it should be noted that considering the equal integer for four types of pedestrians and the system size $W=60$, the data points is few, and the critical entrance density and the critical occupancy are determined as the average of 10 random pedestrian distributions in the entrances of boundaries.

Figure 8 gives the time evolution of (a) the velocity $V(t)$ and (b) the occupancy $\rho(t)$ for the system size $W=60$ in the pedestrian counterflow with open boundary condition at the entrance density $p_o=0.1$, 0.2, and 0.5. Here only give the

first 4000 time steps. For the entrance density $p_o=0.1$ and 0.5, the velocity and occupancy reach quickly the steady values. It should be noted that for $p_o=0.2$, there are two steady states; but the first is metastable. Spontaneous fluctuations can disrupt the freely moving flow forming small jam clusters. And then two situations, which depends on the entrance density and initial pedestrian distribution, may occur. The first is that the system can break up of small clusters when the jammed pedestrians in these clusters succeed in moving past each other, thereby dissolving the clusters. And then the system will stabilize in the freely moving phase. The second is that pedestrians may get jammed with the existing clusters making these clusters grow further with time, and the bigger jam clusters come into being. Eventually the system can run into a jam by this mechanism, which means the system transits to the perfectly stopped phase from the freely moving phase. This phenomenon can be seen in Fig. 9, which is the time evolution of pedestrian patterns obtained at (a) times step=900, (b) 1800, and (c) 2700 for the system size $W=60$ in the pedestrian counterflow with open boundary condition at the entrance density $p_o=0.2$. In the beginning (time step=900), pedestrians can move freely. At some time, small jam clusters form occasionally. We can see there are three small jam clusters at time step=1800 from Fig. 9(b). These clusters grow with time (time step=2700). These emerging clusters show that jamming is mainly caused by oppositely moving pedestrians (white and black vs red and green) getting jammed with each other. Since there is no back step movement, once the oppositely moving pedestrians get jammed they can only move sideways and occasionally forwards. While the already jammed pedestrians try to move out of existing jam clusters, the other moving pedestrians get jammed with the existing clusters making these clusters grow further with time.

IV. CONCLUSIONS

In this paper, a cellular automaton model without step back for pedestrian dynamics considering the human behaviors which can make judgment in some complex situations is presented. This model considers the traffic rule and custom through the different transition probabilities in directions. Pedestrian movement with different walk velocities can be simulated through update at different time-step intervals. Periodic and open boundary conditions for pedestrian counter flow are considered. Simulations show that with the periodic boundary condition, this simple model can reproduce some typical phenomena observed empirically such as lane formation and jamming, etc. For periodic boundary condition there are three phases of pedestrian patterns, i.e., freely moving phase, lane formation phase, and perfectly stopped phase at some certain total density ranges. In the stage of lane formation, this presented model can simulate the phenomenon that pedestrians exceed those with lower walk velocity through a narrow walkway. For open boundary condition, there are two steady states of pedestrian patterns at some certain entrance densities; but the first is metastable. Spontaneous fluctuations can break the first steady state, i.e., freely moving phase, and run into the second steady state, i.e., perfectly stopped phase.

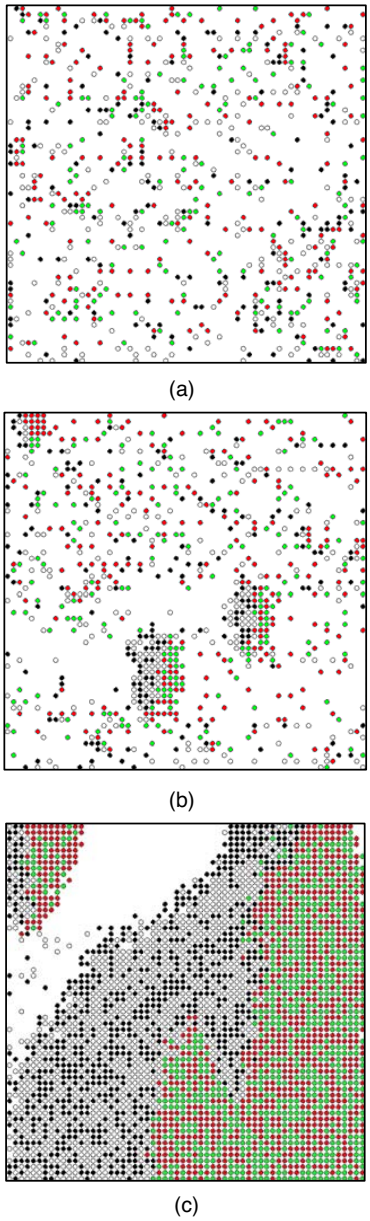

FIG. 9. (Color online) Time evolution of pedestrian patterns obtained at (a) time step=900, (b) 1800, and (c) 2700 for the system size $W=60$ in the pedestrian counter flow with open boundary condition at the entrance density $p_o=0.2$.

ACKNOWLEDGMENTS

The authors would like to acknowledge the supports provided by the China NKBRSF project (Grant No. 2001CB409600).

[1] B. Chopard and M. Droz, *Cellular Automata Modeling of Physical Systems* (Cambridge University Press, Australia, 1998).
[2] M. Fukui and Y. Ishibashi, J. Phys. Soc. Jpn. **65**, 1868 (1996).
[3] J. Matsukidaira and K. Nishinari, Phys. Rev. Lett. **90**, 088701 (2003).
[4] H. K. Lee, R. Barlovic, M. Schreckenberg, and D. Kim, Phys. Rev. Lett. **92**, 238702 (2004).
[5] M. Muramatsu, T. Irie, and T. Nagatani, Physica A **267**, 487 (1999).
[6] M. Muramatsu and T. Nagatani, Physica A **286**, 377 (2000).
[7] Y. Tajima, K. Takimoto, and T. Nagatani, Physica A **294**, 257 (2001).
[8] K. Takimoto and T. Nagatani, Physica A **320**, 611 (2003).
[9] M. Fukui and Y. Ishibashi, J. Phys. Soc. Jpn. **68**, 2861 (1999).
[10] S. Maniccam, Physica A **321**, 653 (2003).
[11] S. Maniccam, Physica A **331**, 669 (2004).
[12] S. Maniccam, Physica A **346**, 631 (2005).
[13] W. F. Fang, L. Z. Yang, and W. C. Fan, Physica A **321**, 633 (2003).
[14] C. Burstedde, K. Klauck, A. Schadschneider, and J. Zittartz, Physica A **295**, 507 (2001).
[15] A. Kirchner and A. Schadschneider, Physica A **312**, 260 (2002).
[16] A. Schadschneider, A. Kirchner, and K. Nishinari, Lect. Notes Comput. Sci. **2493**, 239 (2002).
[17] D. Helbing, I. J. Farkas, and T. Vicsek, Phys. Rev. Lett. **84**, 1240 (2000).
[18] D. Helbing, I. J. Farkas, P. Molnar, and T. Vicsck, in: *Pedestrian and Evacuation Dynamics*, edited by M. Schreckenberg and S. D. Sharma, (Springer, Berlin, 2001).
[19] D. Helbing, I. J. Farkas, and T. Vicsek, Nature (London) **407**, 487 (2000).
[20] D. Helbing and P. Molnar, Phys. Rev. E **51**, 4282 (1995).
[21] O. Biham, A. A. Middleton, and D. Levine, Phys. Rev. A **46**, R6124 (1992).
[22] A. Kirchner, H. Kluepfel, K. Nishinari, A. Schadschneider, and M. Schreckenberg, J. Stat. Mech.: Theory Exp. 2004, P100011 (2004).
[23] M. Wolki, A. Schadschneider, and M. Schreckenberg, J. Phys. A **39**, 33 (2006).
[24] C. B. Bai, Undergraduate thesis, Tsinghua University, 2006 (in Chinese).